

Potential roots of the deep sub-barrier heavy-ion fusion hindrance phenomenon

P. W. Wen,^{1,2} C. J. Lin,^{2,3,*} R. G. Nazmitdinov,^{1,4,†} S. I. Vinitzky,^{1,5,‡} O. Chuluunbaatar,^{1,6} A. A. Gusev,¹ A. K. Nasirov,^{1,7} H. M. Jia,² and A. Gózdź⁸

¹Joint Institute for Nuclear Research, 141980 Dubna, Russia

²China Institute of Atomic Energy, 102413 Beijing, China

³Department of Physics, Guangxi Normal University, 541004 Guilin, China

⁴Dubna State University, 141982 Dubna, Russia

⁵Peoples' Friendship University of Russia (RUDN University), 117198 Moscow, Russia

⁶Institute of Mathematics and Digital Technologies,

Mongolian Academy of Sciences, 13330 Ulaanbaatar, Mongolia

⁷Institute of Nuclear Physics, Ulugbek, 100214, Tashkent, Uzbekistan

⁸Institute of Physics, University of M. Curie-Skłodowska, 520031 Lublin, Poland

(Dated: November 4, 2020)

We analyse the origin of the unexpected deep sub-barrier heavy-ion fusion hindrance in $^{64}\text{Ni}+^{100}\text{Mo}$ and $^{28}\text{Si}+^{64}\text{Ni}$ reactions. Our analysis is based on the improved coupled-channels approach, implemented by means of the finite element method. With the aid of the Woods-Saxon potential the experimental cross sections and the S -factors of these reactions are remarkably well reproduced. We found that the account on the non-diagonal matrix elements of the coupling matrix, traditionally neglected in the conventional coupled-channels approaches in setting the left boundary conditions inside the potential pocket, and its minimal value are crucially important for the interpretation experimental data. Within our approach we found a good agreement with the experimental data for the S -factor of the fusion reaction $^{12}\text{C}+^{12}\text{C}$, which has no a pronounced maximum for this system.

Various stages of astrophysical nucleogenesis, the synthesis of superheavy nuclei, and, consequently, effective mechanisms of nucleus-nucleus interaction [1–6], require a deep understanding of the near barrier heavy-ion fusion reaction. Since 2002 precise measurements have been available to probe the effects of the interaction potential at the deep sub-barrier energies [7]. However, at these energies the fusion cross sections fall off much steeper than the conventional coupled-channels (CC) calculations predict. This unexpected fusion hindrance phenomenon is generally accompanied by the maximum of the astrophysical S -factor. Due to its notable influence on the astrophysical nuclear reaction processes for fusion reactions like $^{12}\text{C}+^{12}\text{C}$ [8–13], this problem is a subject of extensive studies in the past years [7, 14–16].

Since the discovery of the fusion hindrance phenomenon, the consensus is that the conventional CC calculations based on a Woods-Saxon (WS) potential are insufficient to reproduce the experimental data [1, 2, 17]. As a result, numerous theoretical attempts have been developed to tackle this problem. Among them are such as the hybrid of different nuclear potentials [18, 19], the extending of the CC framework to the adiabatic states [20], the quantum diffusion approach [21], the density-constrained frozen Hartree-Fock method [22], to name just a few.

In fact, within the conventional CC approach we can distinguish between two directions of the theoretical ex-

planations for the hindrance mechanisms. The first one is based on the sudden approximation for a hybrid of different potentials. In particular, a gentle overlap of the reacting nuclei is considered due to the saturation properties of nuclear matter [18, 23, 24]. One attempts to explain the steep falloff of fusion cross sections by using the double-folding potential with M3Y forces supplemented by a repulsive core. Another approach analyses the hindrance phenomenon by fitting the fusion excitation function with two separate WS potentials [19]. On different sides of the threshold energy where the maximum of the S -factor locates, the model includes the potentials that produce different logarithmic slope of the excitation functions. The second direction is based on the adiabatic approximation [20, 25]. On the top of the conventional CC method, an extra one-dimensional adiabatic potential barrier is assumed after the reacting nuclei contacts with each other, considering the formation of the composite system. Thus, the mechanism of the deep sub-barrier hindrance is still debatable. In spite of numerous attempts it remains to be a real challenge for nuclear reaction theory. The main goal of the present paper is to explain the unexpected deep sub-barrier heavy-ion fusion hindrance, providing the principle of bounding solutions for the scattering problem of two colliding nuclei, developed in Refs. [26, 27].

We consider the collision between two nuclei, which relative motion is coupled to nuclear intrinsic motion. The potential between the projectile and the target contains the Coulomb potential and nuclear potential, chosen in the WS form $V_N^{(0)}(r) = -V_0/(1 + \exp[(r - R_0)/a_0])$. Here, the parameters V_0 , R_0 , and a_0 are the potential depth, potential radius, and diffuseness, respectively; r

* corresponding author: cjlin@ciae.ac.cn

† corresponding author: rashid@theor.jinr.ru

‡ corresponding author: vinitzky@theor.jinr.ru

is the distance between the mass centers of the two interacting nuclei.

Following Refs. [28, 29]), in our approach the nuclear coupling Hamiltonian is generated by changing the target radius in the potential to the dynamical operator $R_0 + \hat{O}$, which is related to collective vibrations. The solution of the CC equations between values r_{\max} and r_{\min} is found under the incoming wave boundary conditions (IWBC), i.e., it is assumed a strong absorption inside the potential pocket. The right boundary point r_{\max} is usually set at a large enough distance where the interaction is weak, and the off-diagonal elements of the coupling matrix tend to be zero. The r_{\min} is determined at the minimum of the potential pocket V_P .

At the left boundary $r = r_{\min}$, the open left exit channel wave functions are usually taken as the plane wave $\psi_{nn_o}^{(\ell)}(r) = \exp(-ik_n(r_{\min})r)T_{nn_o}^{(\ell)}$, where $T_{nn_o}^{(\ell)}$ is the tunneling amplitude. The definition of $k_n(r_{\min}) = \sqrt{\frac{2\mu}{\hbar^2}E - W_{nn}^{(\ell)}(r_{\min})} > 0$, involves only diagonal elements of the coupling matrix, assuming that the off-diagonal matrix elements tend to be zero (e.g., Refs. [28, 29]). We recall that $W_{nm}^{(\ell)}(r) = \frac{2\mu}{\hbar^2} [V^{(\ell)}(r)\delta_{nm} + V_{nm}(r)]$ at $r > r_{\min}$; and the constant valued matrix $W_{nm} = W_{nm}^{(\ell)}(r_{\min})$ at $r \leq r_{\min}$. Here, $V^{(\ell)}(r) = \frac{Z_P Z_T e^2}{r} + V_N^{(0)}(r) + \frac{\hbar^2 \ell(\ell+1)}{2\mu r^2} + \epsilon_n$ is the potential energy without the coupling. Further, $V_{nm}(r)$ are elements of the coupling matrix, μ is the reduced mass, Z_P and Z_T are the Coulomb charges of projectile and target ions, ℓ is the orbital angular momentum, and ϵ_n is the excitation energy of the n -th entrance channel or the entrance threshold energy $E = \epsilon_n$ at $n = 1, \dots, N$.

It is important to stress that at r_{\min} , the distance between two nuclei becomes so small, that the off-diagonal matrix elements $W_{nn'}^{(\ell)}(r_{\min})$ are usually not zero. As addressed in Refs. [30, 31], there can be sudden noncontinuous changes at the left boundary conditions, and this will distort the total wave function inside the barrier.

To treat properly this problem, at the left boundary we adopt the linear transformation method [26, 27]. Namely, at $r \leq r_{\min}$, when the off-diagonal matrix elements have been taken into account, the modified solutions of the CC equations $\tilde{\psi}_{nn_o}^{(\ell)}(r)$ consist of the linear independent solutions $\phi_{nm}^{(\ell)}(r)$, i.e., $\tilde{\psi}_{nn_o}^{(\ell)}(r) = \sum_{m=1}^{M_o} \phi_{nm}^{(\ell)}(r)\tilde{T}_{mn_o}^{(\ell)}$. In this case the linear independent matrix solution can be obtained by considering the transformation $\phi_{nm}(r) = A_{nm}y_m(r)$, where $y_m(r)$ are solutions of the uncoupled equations

$$y_m''(r) + K_m^2 y_m(r) = 0, K_m^2 = (2\mu/\hbar^2)E - \tilde{W}_{mm}.$$

Here, \mathbf{A} and $\tilde{\mathbf{W}}$ are the matrix of eigenvectors and the diagonal matrix of eigenvalues of the eigenvalue problem, respectively. In short, we diagonalize the coupling matrix $\mathbf{A}^{-1}\mathbf{W}\mathbf{A} = \tilde{\mathbf{W}}$. For the open channels with $K_m^2 > 0$, $y_m(r) = \exp(-iK_m r)/\sqrt{K_m}$ at $m = 1, \dots, M_o \leq N$. The partial fusion probability $P_{n_o}^{(\ell)} = \sum_{m=1}^{M_o} |\tilde{T}_{mn_o}^{(\ell)}|^2 \neq$

TABLE I. Woods-Saxon potential parameters V_0 (MeV), a_0 (fm), R_0 (fm) for $^{64}\text{Ni}+^{100}\text{Mo}$, and $^{28}\text{Si}+^{64}\text{Ni}$ reaction systems. The potential barrier V_B and the minimum of the potential pocket V_P are also listed.

	$^{64}\text{Ni}+^{100}\text{Mo}$	$^{28}\text{Si}+^{64}\text{Ni}$
V_0 (MeV)	79.938	62.707
a_0 (fm)	0.686	1.014
R_0 (fm)	10.190	7.354
V_B (MeV)	136.993	52.697
V_P (MeV)	119.344	43.027

$\sum_{m=1}^{M_o'} |T_{mn_o}^{(\ell)}|^2$ is given by summing over all open exit channels at $r \leq r_{\min}$. We stress that the number of open channels after and before the diagonalization of the coupling matrix will be different. At $r \geq r_{\max}$ the asymptotic solutions are given in terms of the normalized Coulomb functions with the wave number $k_n = \sqrt{\frac{2\mu}{\hbar^2}(E - \epsilon_n)} > 0$ in the entrance n_o and the right exit n open channels $n_o, n = 1, \dots, N_o \leq N$ and the reflection amplitudes $\tilde{R}_{nn_o}^{(\ell)}$ [27].

To illuminate all cons and pros of our approach we re-examine $^{64}\text{Ni}+^{100}\text{Mo}$, and $^{28}\text{Si}+^{64}\text{Ni}$ reactions. To this aim we analyse the fusion cross sections $\sigma = \sigma_{\text{fus}}(E) = \sum_{\ell=0}^{\ell_{\max}} \sigma_{\ell}(E) = \frac{\pi}{k_{n_o}^2} \sum_{\ell=0}^{\ell_{\max}} (2\ell+1)P_{n_o}^{(\ell)}(E)$ and the astrophysical S factor (see Fig. 1). Our results have been obtained with the aid of the KANTBP code, developed by means of the finite element method (see for details Refs. [32–36]) for the set $N = 1 + N_{\text{coupl}}$ of CC equations with the improved IWBC from the corresponding ground states $|n_o - 1 = 0\rangle$. The number of all channels N_{coupl} depends of the chosen reaction. It is noteworthy that, using the program KANTBP, the sum of tunneling and reflection probabilities $\sum_{m=1}^{M_o} |\tilde{T}_{mn_o}^{(\ell)}|^2 + \sum_{n=1}^{N_o} |\tilde{R}_{nn_o}^{(\ell)}|^2 - 1 \simeq 10^{-10}$. It is the stringiest test of the validity of our calculations.

The coupling radius parameter for the collective vibrations is set to be 1.2 fm for all the cases in this study [26]. Note, that the value of ℓ_{\max} is restricted by the constraint on the incident energy values E in the entrance channel: $E = V^{(\ell)}(r_{\min})$, where $V^{(\ell)}(r_{\min})$ is the potential minimum, and $\ell = 0, \dots, \ell_{\max}$. The values of η_0 used for scaling the astrophysical factor $S(E) = E\sigma_{\text{fus}}(E)\exp(2\pi(\eta - \eta_0))$ for the above three reactions are 105.74, 75.23, and 41.25, respectively; η is the Sommerfeld parameter. The adopted structure properties (including excitation energies, deformation parameters for the collective state) are taken from Refs. [37, 38]. The potential parameters in this study are obtained by fitting the experimental fusion data at the whole energy region with the CC calculations and the simple WS potential (see Table I).

There is a remarkable agreement between our calculations and available experimental data for the fusion cross sections and S -factors (see Fig. 1). Note, that all

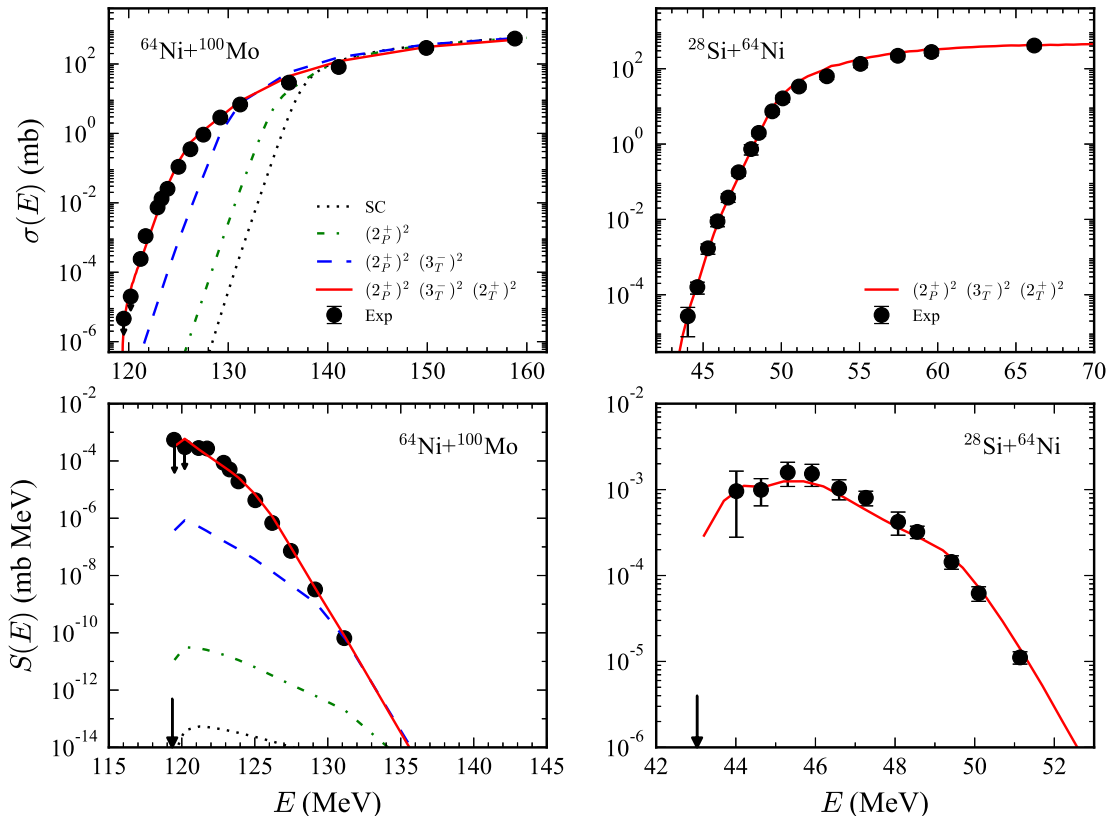


FIG. 1. (Color online) The fusion cross sections $\sigma(E)$ and the astrophysical $S(E)$ -factor for $^{64}\text{Ni}+^{100}\text{Mo}$ and $^{28}\text{Si}+^{64}\text{Ni}$ reaction systems. Different curves denote the CC calculations with different sets of collective vibrations, indicated by the legends; the SC means a single-channel calculations (without coupling). The experimental data (solid circles) are taken from Ref. [14] and Ref. [16], respectively. The black arrows indicate the potential pocket minimum V_P .

S -factors of these reactions have maxima. To explore the general reason for the hindrance and the maximum of the S -factor, we consider also the results for different combinations of the collective vibrations for $^{64}\text{Ni}+^{100}\text{Mo}$ (see Fig. 1). All calculations for various number of coupled channels demonstrate as well the maximum for S -factor, including the single-channel case (SC) when all $V_{nm}(r) \equiv 0$ (i.e. without couplings). We observe that the energies, where the hindrance and the maximum of S -factor take place, are close to the potential pocket minimum V_P for different couplings.

Although the importance of the potential pocket minimum in the CC calculations was already noticed in Refs. [18, 23, 39], the agreement between experimental data and the results of calculations was not reached. In these studies the repulsive core inside the shallow potential pocket was suggested as one of the reasons for the hindrance phenomenon. To find out why the hindrance and the maximum of S -factor happen always near V_P , we compare the CC results without and with the diagonalization for $^{64}\text{Ni}+^{100}\text{Mo}$ [see Fig. 2 (a)]. It appears that the correct treatment of the left boundary is one of the decisive factors, that allows to reach a good agreement

with the experiment, using the simple WS potential.

To gain further insight into the details of the hindrance phenomenon, we compare the mean angular momentum $\langle \ell \rangle = \sum_{\ell=0}^{\ell_{max}} \ell \sigma_{\ell}(E) / \sigma(E)$ (see also Ref. [40]) for the complete calculations and without coupling [see Fig. 2 (b)]. Note, that when $E \rightarrow V_P$, the $\langle \ell \rangle$ decreases to zero quickly if there is the constraint on the energy for both cases. In this case, the energy is too small, and only the s -wave partial contribution determines the cross section. It seems, that to obtain a good agreement with the experimental data, the constraint is important as well [compare Figs. 2 (a), (b)]. At $E > V_P$ there are many coupled channels at the complete calculations, and, consequently, the barrier has a certain kind of distribution, which obscures the barrier position.

To elucidate further the basic mechanism of the hindrance factor in our calculations, we compare the potential energy $V(r)$ (without coupling), the diagonal elements $\hbar^2 \mathbf{W}_{nn} / 2\mu$ of the coupled matrix, and the threshold energies $\hbar^2 \tilde{\mathbf{W}}_{nn} / 2\mu$ at the left boundary (see Fig. 3). As it is seen, the threshold energies $\hbar^2 \tilde{\mathbf{W}}_{nn} / 2\mu$ spread much wider than the diagonal elements $\hbar^2 \mathbf{W}_{nn} / 2\mu$ of the

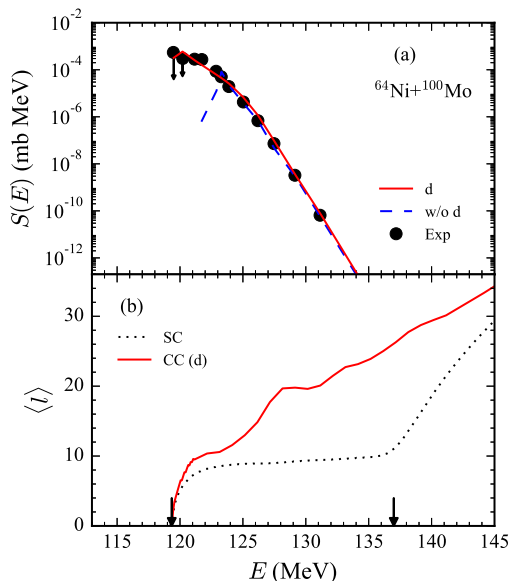


FIG. 2. (Color online) The astrophysical $S(E)$ -factor and the mean orbital momentum $\langle \ell \rangle$ for the reaction ${}^{64}\text{Ni}+{}^{100}\text{Mo}$. Panel (a): the results of the CC calculations with the diagonalization (solid line) and without the diagonalization (dashed line) are compared with the experimental data (full circle) [see text for details]. Panel (b): the mean orbital momentum $\langle \ell \rangle$ for the single channel (without coupling) (dotted line) and for the full coupling (solid line) with the diagonalization procedure. The arrows indicate the position of the potential barrier V_B and the pocket minimum energy V_P .

coupled matrix. Especially, the minimum threshold energy of $\hbar^2\tilde{\mathbf{W}}_{11}/2\mu$ is obviously much lower V_P . In other words, in contrast to the conventional CC calculations, in our approach the number of open channels is much larger.

It appears that the experimental fusion cross section can be reproduced well only under certain physical couplings. For these reactions, the entanglement between the states at the left boundary is changed through the diagonalization procedure. On the other hand, in the CC calculations, when the incident energy $E < V_P = V^{(\ell=0)}(r_{min})$, the tunneling is absent. It is due the fact that the ingoing flux will be zero [23, 28, 39]. Thus, when the incident energy gradually approaches the bottom of the potential pocket minimum, the fusion hindrance occurs naturally.

Let us turn to the most important fusion reaction ${}^{12}\text{C}+{}^{12}\text{C}$ in nuclear astrophysics within our approach. We recall that the carbon fusion plays a significant role in the burning of the massive stars, ignition of the type Ia supernovae explosion, superbursts of binary systems or neutron stars [2]. It remains an open problem whether the fusion hindrance does, indeed, occur in this reaction, which is closely related to the astrophysical reaction rate [8, 13].

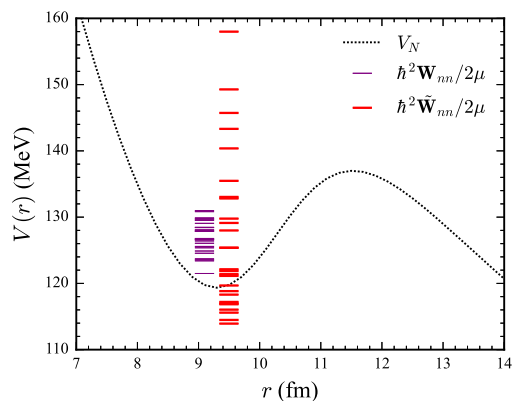


FIG. 3. (Color online) The potential $V(r)$ (dotted line), diagonal matrix elements of the coupled matrix $\hbar^2\mathbf{W}_{nn}(r_{min})/2\mu$ (thin solid lines) and eigenvalues $\hbar^2\tilde{\mathbf{W}}_{nn}(r_{min})/2\mu$ (thick solid lines) for the case of ${}^{64}\text{Ni}+{}^{100}\text{Mo}$. See text for details.

As above, we fit the experimental fusion cross section [8] with the aid of the WS potential: $V_0 = 34.252$ MeV, $R_0 = 3.865$ fm, and $a_0 = 0.952$ fm. In addition, we consider the quadrupole excitations. In this case the fusion cross section is defined as $\sigma(E) = 2 \sum_{\ell=\text{even}}^{\ell_{max}} \sigma_{\ell}(E)$. For the carbon fusion, we adopt the commonly used definition $S^*(E) = \sigma(E) \cdot E \cdot \exp(87.21/\sqrt{E} + 0.46E)$ [10, 12]. The results of calculations with and without the diagonalization demonstrate a good agreement with experimental fusion data [8, 10]. In contrast to the results shown in Fig.1, where the $S(E)$ factor drops at low energy tail region evidently, the $S^*(E)$ -factor evolve smoothly with the decreasing energy. It should be noted that the trend of the $S^*(E)$ -factor over the energy E is different from that for the $S(E)$ -factor. At low energy region, $S^*(E)$ is lower than that of $S(E)$. And for the $S^*(E)$ -factor, the calculations indicate that there are no clear decrease and the maximum for this system at low energies. Note, that our results are similar to those of the CC theory with M3Y+repulsive core potential in Ref. [24].

In our calculations, based on the WS potential, the reason for the steady trend can be traced from Fig. 4a. The threshold energies after the diagonalization change modestly in the comparison with those without the diagonalization. The bottom of the potential pocket is about -7 MeV, which is far from the incident energy region of interest (about 1.5-3 MeV). Therefore, the hindrance feature is not so obvious as that seen in Fig. 1. In the former case the S^* factor changes slowly below the potential barrier.

Surprisingly, we find that our results are supported by the empirical trends, discussed for the hindrance factor in Ref. [41]. Indeed, our results for the medium nuclei manifest the hindrance factor for system with $Z_1Z_2\sqrt{\mu} \geq 2000$. While for the lightest system with $Z_1Z_2\sqrt{\mu} \leq 200$ the logarithmic slopes of the $S^*(E)$ factor exhibits resistance to the increasing tendency with

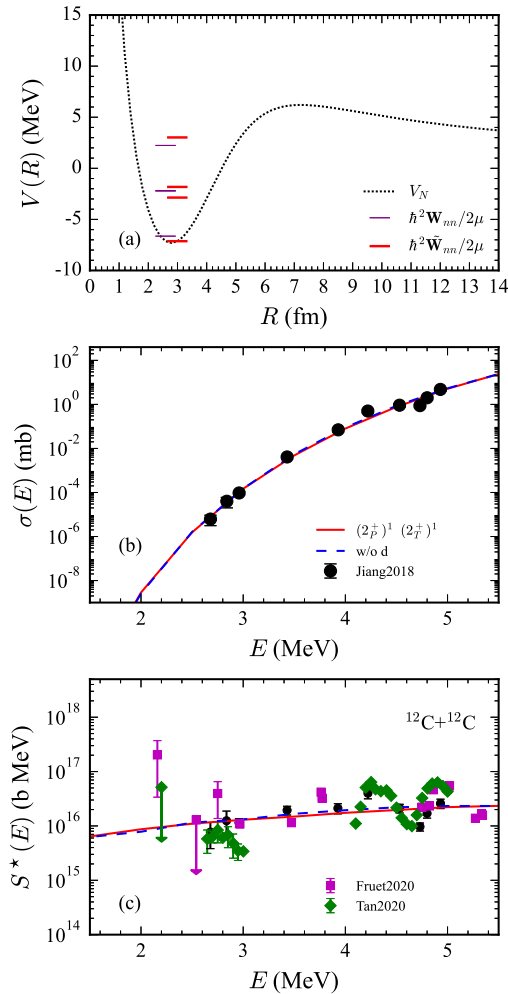


FIG. 4. (Color online) (a) Similar to Fig.3 for the case of $^{12}\text{C}+^{12}\text{C}$. (b) The results for the fusion cross sections $\sigma(E)$ with the diagonalization (solid line) and without the diagonalization (dashed line). (c) The results for the $S^*(E)$ -factor with the diagonalization (solid line) and without the diagonalization (dashed line). The experimental data labeled as Jiang2018, Tan2020, Fruet2020, are taken from Refs. [8], Ref. [10], Ref. [11], respectively. All results are obtained with the indicated collective vibrations.

the energy. In our approach the variation of the coupling strength of the left exit channels is the basic mechanism, responsible for the observed phenomenon. The coupling strength is much stronger for the medium and heavy sys-

tem, while it is much weaker for the lightest systems. In other words, the degree of the strength controls the number of open channels, contributing to the reaction.

In summary, the deep sub-barrier heavy-ion fusion hindrance phenomenon and the behavior of the astrophysical S -factor for $^{64}\text{Ni}+^{100}\text{Mo}$, and $^{28}\text{Si}+^{64}\text{Ni}$ reactions are analysed by solving the CC equations with the improved IWBC. This approach has been developed in Refs. [26, 27] and based on the finite element method KANTBP [32–36]). The obtained results reproduce remarkably well the experimental data with the aid of the simple WS potential. It is found that the calculated S -factors with different kinds of collective vibrations have maxima for the considered reactions. The knowledge of the potential minimum energy V_P and the improved IWBC are crucially important for the correct interpretation of the fusion cross section in the conventional CC calculations. The general trend of the directly measured fusion data for the reaction $^{12}\text{C}+^{12}\text{C}$ [8, 10] is described as well. It is found that the S^* factor drops gently at energies under the Coulomb barrier, and the results show no a pronounced maximum of the S^* -factor for this system. We hope that further experiments at low energies could finally reveal "the mystery of the hindrance phenomenon" as a function of the mass number. From our point of view it is simply determined by the number of coupled channels at the correct treatment of the left boundary conditions for different combinations of the colliding nuclei.

ACKNOWLEDGEMENTS

The work of P.W.W., C.J.L., and H.M.J. is supported by the National Natural Science Foundation of China (Grants Nos. 11635015, 11805120, 11635003, 11805280, 11811530071, U1867212 and U1732145), the National Key R&D Program of China (Contract No. 2018YFA0404404), and the Continuous Basic Scientific Research Project (No.WDJC-2019-13). The present research benefited from computational resources of the HybridLIT heterogeneous platform of the JINR. This work was partially supported by the Polish–French COPIN collaboration of the project 04–113, the Bogoliubov–Infeld and the Hulubei–Meshcheryakov JINR programs, the grant RFBR and MECSS 20–51–44001, the grant RFBR 17-52-45037, the RUDN University Program 5–100 and grant of Plenipotentiary of the Republic of Kazakhstan in JINR.

[1] G. Montagnoli and A. M. Stefanini, *Eur. Phys. J. A* **53**, 169 (2017).

[2] B. B. Back, H. Esbensen, C. L. Jiang, and K. E. Rehm, *Rev. Mod. Phys.* **86**, 317 (2014).

[3] C. J. Lin, *Heavy-ion nuclear reactions* (Harbin Engineering University Press, Harbin, 2015).

[4] L. Yang, C. J. Lin, H. M. Jia, D. X. Wang, N. R. Ma, L. J. Sun, F. Yang, X. X. Xu, Z. D. Wu, H. Q. Zhang, and Z. H. Liu, *Phys. Rev. Lett.* **119**, 042503 (2017).

- [5] H. M. Jia, C. J. Lin, L. Yang, X. X. Xu, N. R. Ma, L. J. Sun, F. Yang, Z. D. Wu, H. Q. Zhang, Z. H. Liu, and D. X. Wang, *Phys. Lett. B* **755**, 43 (2016).
- [6] A. K. Nasirov, B. M. Kayumov, G. Mandaglio, G. Giardina, K. Kim, and Y. Kim, *Eur. Phys. J. A* **55**, 29 (2019).
- [7] C. L. Jiang, H. Esbensen, K. E. Rehm, B. B. Back, R. V. F. Janssens, J. A. Caggiano, P. Collon, J. Greene, A. M. Heinz, D. J. Henderson, I. Nishinaka, T. O. Pennington, and D. Seweryniak, *Phys. Rev. Lett.* **89**, 052701 (2002).
- [8] C. L. Jiang, D. Santiago-Gonzalez, S. Almaraz-Calderon, K. E. Rehm, B. B. Back, K. Auranen, M. L. Avila, A. D. Ayangeakaa, S. Bottoni, M. P. Carpenter, C. Dickerson, B. DiGiovine, J. P. Greene, C. R. Hoffman, R. V. F. Janssens, B. P. Kay, S. A. Kuvin, T. Lauritsen, R. C. Pardo, J. Sethi, D. Seweryniak, R. Talwar, C. Ugalde, S. Zhu, D. Bourgin, S. Courtin, F. Haas, M. Heine, G. Fruet, D. Montanari, D. G. Jenkins, L. Morris, A. Lefebvre-Schuhl, M. Alcorta, X. Fang, X. D. Tang, B. Bucher, C. M. Deibel, and S. T. Marley, *Phys. Rev. C* **97**, 012801 (2018).
- [9] A. Tumino, C. Spitaleri, M. La Cognata, S. Cherubini, G. L. Guardo, M. Gulino, S. Hayakawa, I. Indelicato, L. Lamia, H. Petrascu, R. G. Pizzone, S. M. R. Puglia, G. G. Rapisarda, S. Romano, M. L. Sergi, R. Spart, and L. Trache, *Nature* **557**, 687 (2018).
- [10] W. P. Tan, A. Boeltzig, C. Dulal, R. J. deBoer, B. Frentz, S. Henderson, K. B. Howard, R. Kelmar, J. J. Kolata, J. Long, K. T. Macon, S. Moylan, G. F. Peaslee, M. Renaud, C. Seymour, G. Seymour, B. Vande Kolk, M. Wiescher, E. F. Aguilera, P. Amador-Valenzuela, D. Lizzano, and E. Martinez-Quiroz, *Phys. Rev. Lett.* **124**, 192702 (2020).
- [11] G. Fruet, S. Courtin, M. Heine, D. G. Jenkins, P. Adsley, A. Brown, R. Canavan, W. N. Catford, E. Charon, D. Curién, S. Della Negra, J. Duprat, F. Hammache, J. Lesrel, G. Lotay, A. Meyer, D. Montanari, L. Morris, M. Moukaddam, J. Nippert, Z. Podolyk, P. H. Regan, I. Ribaud, M. Richer, M. Rudigier, R. Shearman, N. de Srville, and C. Stodel, *Phys. Rev. Lett.* **124**, 192701 (2020).
- [12] Y. J. Li, X. Fang, B. Bucher, K. A. Li, L. H. Ru, and X. D. Tang, *Chin. Phys. C* (accepted) (2020).
- [13] C. Beck, A. M. Mukhamedzhanov, and X. Tang, *Eur. Phys. J. A* **56**, 87 (2020).
- [14] C. L. Jiang, K. E. Rehm, H. Esbensen, R. V. F. Janssens, B. B. Back, C. N. Davids, J. P. Greene, D. J. Henderson, C. J. Lister, R. C. Pardo, T. Pennington, D. Peterson, D. Seweryniak, B. Shumard, S. Sinha, X. D. Tang, I. Tanihata, S. Zhu, P. Collon, S. Kurtz, and M. Paul, *Phys. Rev. C* **71**, 044613 (2005).
- [15] M. Dasgupta, D. J. Hinde, A. Diaz-Torres, B. Bouriquet, C. I. Low, G. J. Milburn, and J. O. Newton, *Phys. Rev. Lett.* **99**, 192701 (2007).
- [16] C. L. Jiang, B. B. Back, H. Esbensen, R. V. F. Janssens, Ş. Mişicu, K. E. Rehm, P. Collon, C. N. Davids, J. Greene, D. J. Henderson, L. Jisonna, S. Kurtz, C. J. Lister, M. Notani, M. Paul, R. Pardo, D. Peterson, D. Seweryniak, B. Shumard, X. D. Tang, I. Tanihata, X. Wang, and S. Zhu, *Phys. Lett. B* **640**, 18 (2006).
- [17] C. L. Jiang, K. E. Rehm, R. V. F. Janssens, H. Esbensen, I. Ahmad, B. B. Back, P. Collon, C. N. Davids, J. P. Greene, D. J. Henderson, G. Mukherjee, R. C. Pardo, M. Paul, T. O. Pennington, D. Seweryniak, S. Sinha, and Z. Zhou, *Phys. Rev. Lett.* **93**, 012701 (2004).
- [18] Ş. Mişicu and H. Esbensen, *Phys. Rev. Lett.* **96**, 112701 (2006).
- [19] K. Hagino, A. B. Balantekin, N. W. Lwin, and E. S. Z. Thein, *Phys. Rev. C* **97**, 034623 (2018).
- [20] T. Ichikawa, K. Hagino, and A. Iwamoto, *Phys. Rev. Lett.* **103**, 202701 (2009).
- [21] V. V. Sargsyan, G. G. Adamian, N. V. Antonenko, and H. Lenske, *Eur. Phys. J. A* **56**, 19 (2020).
- [22] C. Simenel, A. S. Umar, K. Godbey, M. Dasgupta, and D. J. Hinde, *Phys. Rev. C* **95**, 031601 (2017).
- [23] Ş. Mişicu and H. Esbensen, *Phys. Rev. C* **75**, 034606 (2007).
- [24] H. Esbensen, X. Tang, and C. L. Jiang, *Phys. Rev. C* **84**, 064613 (2011).
- [25] T. Ichikawa, K. Hagino, and A. Iwamoto, *Phys. Rev. C* **75**, 064612 (2007).
- [26] P. W. Wen, O. Chuluunbaatar, A. A. Gusev, R. G. Nazmitdinov, A. K. Nasirov, S. I. Vinitzky, C. J. Lin, and H. M. Jia, *Phys. Rev. C* **101**, 014618 (2020).
- [27] S. I. Vinitzky, P. W. Wen, A. A. Gusev, O. Chuluunbaatar, R. G. Nazmitdinov, A. K. Nasirov, C. J. Lin, H. M. Jia, and A. Gózdź, *Acta Phys. Polonica B Proc. Suppl.* **101**, 549 (2020).
- [28] K. Hagino, N. Rowley, and A. T. Kruppa, *Comput. Phys. Commun.* **123**, 143 (1999).
- [29] K. Hagino and N. Takigawa, *Prog. Theor. Phys.* **128**, 1061 (2012).
- [30] V. I. Zagrebaev and V. V. Samarin, *Phys. Atom. Nucl.* **67**, 1462 (2004).
- [31] V. V. Samarin and V. I. Zagrebaev, *Nucl. Phys. A* **734**, E9 (2004).
- [32] O. Chuluunbaatar, A. A. Gusev, A. G. Abrashkevich, A. Amaya-Tapia, M. S. Kaschiev, S. Y. Larsen, and S. I. Vinitzky, *Comput. Phys. Commun.* **177**, 649 (2007).
- [33] O. Chuluunbaatar, A. A. Gusev, S. I. Vinitzky, and A. G. Abrashkevich, *Comput. Phys. Commun.* **179**, 685 (2008).
- [34] A. A. Gusev, O. Chuluunbaatar, S. I. Vinitzky, and A. G. Abrashkevich, *Comput. Phys. Commun.* **185**, 3341 (2014).
- [35] A. A. Gusev, O. Chuluunbaatar, S. I. Vinitzky, and A. G. Abrashkevich, *Math. Mod. Geom.* **3**, 22 (2015).
- [36] G. Chuluunbaatar, A. A. Gusev, O. Chuluunbaatar, S. I. Vinitzky, and L. Le Hai, *EPJ Web Conf.* **226**, 02008 (2020).
- [37] S. Raman, C. W. Nestor, and P. Tikkanen, *Atom. Data. Nucl. Data.* **78**, 1 (2001).
- [38] T. Kibédi and R. H. Spear, *Atom. Data. Nucl. Data.* **80**, 35 (2002).
- [39] G. Montagnoli, A. M. Stefanini, H. Esbensen, C. L. Jiang, L. Corradi, S. Courtin, E. Fioretto, A. Goasduff, J. Gregosz, F. Haas, M. Mazzocco, C. Michelagnoli, T. Mijatovic, D. Montanari, C. Parascandolo, K. E. Rehm, F. Scarlassara, S. Szilner, X. D. Tang, and C. A. Ur, *Phys. Rev. C* **87**, 014611 (2013).
- [40] K. Hagino, N. Takigawa, M. Dasgupta, D. J. Hinde, and J. R. Leigh, *Phys. Rev. C* **55**, 276 (1997).
- [41] C. L. Jiang, B. B. Back, H. Esbensen, R. V. F. Janssens, and K. E. Rehm, *Phys. Rev. C* **73**, 014613 (2006).